

# Implementation of a Biologically Inspired Diffusive Filling-In Algorithm for Focal-Plane Image Processing Applications

Genildo Nonato Santos and José Gabriel Rodriguez Carneiro Gomes.  
Universidade Federal do Rio de Janeiro  
PADS / PEE / COPPE / UFRJ  
Rio de Janeiro, Brazil  
gennonato@gmail.com, gabriel@pads.ufrj.br

**Abstract**— The investigation of electronic devices as a replacement for the biological retina has achieved considerable interest over the last years. Tests of retinal prostheses in living patients have led to encouraging results. Such devices can be thought of as image sensors which are created with CMOS technology. Thanks to CMOS fabrication techniques, signal processing hardware can be integrated at the same silicon area where the light sensors are located. The signals generated on the retina are used by different neural mechanisms which are responsible for visual perception, motion detection, depth map construction, and so forth. The knowledge of how these neural mechanisms work, and how they interact with the retina, will enable the development of prostheses for parts of the neural visual system beyond the retina. An interesting feature of the visual system which has not been exploited in terms of hardware is the *diffusive filling-in* mechanism. It is believed that this mechanism enables the perceptual reconstruction of surfaces. In this work we investigate the implementation of the filling-in mechanism details. Our goal is to gather information that will be useful for the development of hardware devices with features similar to those found in this visual perception mechanism.

**Keywords**— difference-of-gaussian filter; computer vision; blind spot; diffusive filling-in process; perceptual reconstruction.

## I. INTRODUCTION

Many hardware devices that perform biologically-inspired image processing tasks have been recently developed. Approximations to the retinal system itself have been implemented in hardware [1], as well as approximations to the motion detection and orientation selectivity algorithms that are present in living neural systems [2, 3]. To theoretically back up the development of these devices, many models for early visual system functionalities have also been presented so far [4, 5, 6]. Most models are based on the *difference-of-gaussian* (DoG) idea, which was first presented by Rodieck [5]. It is

well known that DoG filtering in general causes losses in the acquired data [6]. Furthermore, in early visual system there is a retinal area where no data is available. This area is usually referred to as the *blind spot*. Although DoG filtering and the blind spot are responsible for significant loss of information in the early vision stage, our visual perception of the physical world remains regular, continuous and apparently lossless.

An early visual system model known as the *retino-morphic chip* was implemented in silicon [2]. In that chip, photoreceptors generate electric signals that are proportional to the light intensity  $I$  (Fig. 1) they are exposed to. A DoG filter arises from the lateral connections among circuit building blocks that approximate the behavior of biological cells known as *horizontal cells*. Other biological structures, known as *bipolar cells*, encode the DoG( $I$ ) results into two complementary channels, labeled *on* and *off*, according to the polarity (positive or negative) of these results. Still in that chip, there is a block that mimics the behavior of bipolar cells and hence separates the DoG results into two channels. Both channels go on to subsequent processing blocks that mimic the biological behavior of the *ganglion cells*. Such cells convert their input information into a pulsed representation known as spike train. The reason for implementing this entire system in silicon is the possibility of creating devices that have an interface with biological visual systems, which leads to new research possibilities. To further investigate this interface, one must understand details of the neural spike train processing. Figure 1 illustrates the fact that the tasks that take place at the primary visual system cause significant discontinuities to the

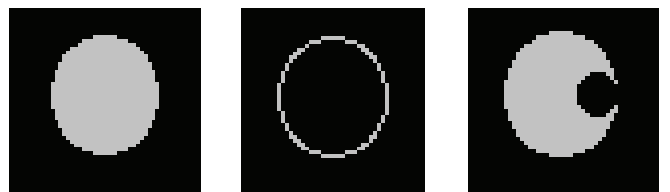


**Figure 1.** Original luminance information (left); information loss due to DoG filtering (center); information loss caused by the blind spot (right).

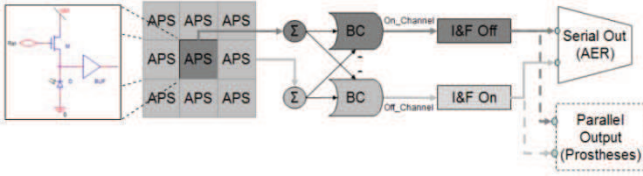


**Figure 2.** Schematic representation of the silicon retina.

visual information. For instance, if  $I$  is related to a gray circle, then it is filled with a black outside and it has a gray inside (as shown in the left part of Fig. 1). The response of the *on* channel can be seen in the center of Fig. 1. This response, which goes to higher-level visual processing areas, is an incomplete version of  $I$ . And, because of the absence of photoreceptors at the blind spot, an additional information loss occurs as illustrated by the right part of Fig. 1. The information loss at the early visual system and the existence of a blind spot in the human retina would lead our external environment perception to be discontinuous. But higher-level visual system mechanisms enable the perception of continuous surfaces where there is none, even if this perception corresponds to an illusion. Visual information recovery tasks are usually associated with mechanisms implemented at the visual cortex. Operations that are related to the visual cortex region are complex and not amenable to silicon implementation. Among these operations, orientation selectivity is particularly difficult. As an example, a hardware device that uses two FPGAs for the implementation of visual cortex orientation tuning was shown in [3]. See also [13] for a digital implementation of similar orientation filters. An additional complexity factor is the fact that the cortical layers of the visual system operate in *integrate-and-fire* (IF) [15] mode which, from a computation point of view, is described using complicated pulse sequences. In this work, we propose an idea for the implementation of a cortical *diffusive filling-in algorithm* (to be detailed in Sec. III) that is suitable for integration with a CMOS image sensor operating in IF mode. We also aim at gathering information that will be useful for the hardware realization of this algorithm. Up to our knowledge, hardware implementations of filling-in algorithms have not been developed so far. We do not consider, at this point, the large complexity that is usually associated with the hardware implementation of cortical mechanisms.

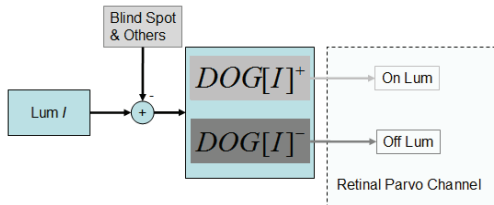


**Figure 3.** Silicon retina functionalities. The *On Lum* and *Off Lum* signals are proportional to those found in the parvocellular channel and, jointly, compose input information for the visual cortex.

Instead, we focus on the filling-in mechanisms and on their interactions with data coming out from the retina. The algorithm presented in [6, 7] will serve as a starting point for our study. The remainder of this paper is structured as follows: a general overview of the processes associated with early vision is presented in Sec. II; the diffusive filling-in algorithm is described in Sec. III; some details of the IF operation mode are given in Sec. IV; Sec. V shows numerical results, and Sec. VI contains our conclusions.

## II. OVERVIEW: FROM RETINA TO DIFFUSIVE FILLING-IN

In this article, we focus on the analysis of diffusive filling-in, an algorithm which may recover some of the brightness information that has been lost by the early visual system circuits. For self-completeness, this section presents context information that is introductory to the filling-in analysis. To establish grounds for the development of a device that can interact with the early visual system or with the post-processing stages of a biological visual system [9], we consider the development of a modified version of the retinomorphic system that was described in [2]. Figure 2 shows a schematic diagram of silicon retina that we consider. An array of pixels (active-pixel sensor structures) interact with bipolar cells and with themselves in order to generate complementary *on* and *off* channels. These channels are then encoded into spikes by IF blocks and sent to an address-event representation (AER) device [12]. Image intensity is inversely proportional to the inter-spike interval and the read-out event associated with each spike is initiated by the pixel. If a parallel output connection is taken directly from the IF *on/off* outputs (i.e. before the AER block as in Fig. 2), then the structure resembles a rudimentary retinal prostheses. The main function of the silicon retina is to generate *on/off* signals that have been degraded by a DoG filter, and to encode them into two spike trains represented in AER mode. Figure 3 shows a block diagram of the silicon retina functionalities. The luminance information  $Lum I$  is degraded by the blind spot and by blood vessels. Then, it is filtered through the DoG operation. The positive (DoG(I)+) and negative (DoG(I)-) response parts compose the *retinal parvo* channel (see Fig. 3), with two components: *On Lum* and *Off Lum*. A post-processing system will receive the signals generated in the early vision stage, and then process those signals according to the perceptual vision scheme outlined in Fig. 4 (schematic model of post processing block), which also shows the diffusive filling-in algorithm.

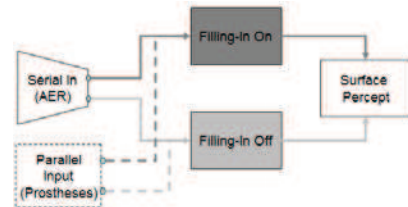


**Figure 4.** Post-processing stage including filling-in algorithm.

### III. ALGORITHM

A diffusive filling-in algorithm based on biological inspiration was presented in [7]. That paper suggests the existence of an information diffusion process among neighboring cells in the visual system. In this process, labeled as diffusive filling-in, areas where visual information has been maintained may complete nearby areas where information was lost. So the process spreads featural qualities (brightness or color) across the perceptual domain.

Two types of perceptual process work together to synthesize a final visual percept in diffusive filling-in: *featural filling-in* and *boundary completion*. Featural filling-in triggers a filling process by which brightness and color signals are spread until they reach their contour limits. Contour limits are formed by signals from the *boundary completion system*. Figure 5 illustrates the diffusive filling-in process. The visual luminance perception (*Percept Lum*) arises when the *on* and *off* filling-in signals are combined, and the diffusion of these signals is limited by the *on/off boundary contour signals*.

#### A. Featural Filling-In

Featural filling-in is the process by which the visual system generates its perception of a surface. The process starts from cells which are within the perceptual domain and are carrying the brightness information. A discrete diffusion equation is indicated in [10] as a model for the filling-in process and, in [11], a similar equation is analyzed with an emphasis on its surface reconstruction features. For simplification, we will use a compact version of the diffusion equation from [10]:

$$D_{45} = \begin{bmatrix} 0 & 0 & 1 \\ 0 & 0 & 0 \\ 0 & 0 & 0 \end{bmatrix}; D_{-45} = \begin{bmatrix} 0 & 0 & 0 \\ 0 & 0 & 0 \\ 0 & 0 & 1 \end{bmatrix}$$

$$F(x) = \sum_k \frac{(x * D_k)^2}{\sum_i x * D_i} \quad (1)$$

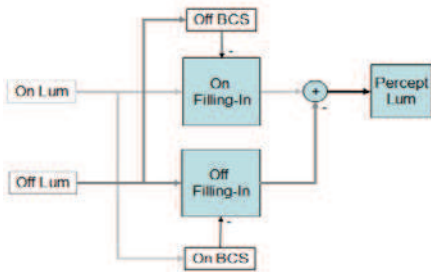


**Figure 5.** Diffusive filling-in block diagram. The filling-in *on/off* signals combine to form the visual perception signal.

In Eq. (1), the matrices  $D_k$  represent masks similar to the sample masks  $D_{45}$  and  $D_{-45}$ , and the  $k$  index indicates the orientation along which diffusion is occurring. The sum of  $D_k$  over  $k$  represents the sum of  $D$  along all orientations. The equation defining  $F(x)$  is called a *diffusion equation*, and  $x$  is an input signal. The expression  $x * D$  denotes the convolution operation between  $x$  and  $D$ . In the original version of the diffusion equation [10], the process is attenuated as the flow moves away from the source. In Eq. (1), no attenuation is applied to the flow. In the algorithm execution, the diffusion flow is trapped within the correct perceptual domain by means of the boundary completion signals. In pixels where there is no boundary signal, the diffusion flow does not stop. In Fig. 6, we used Eq. (1) to generate the response that is expected from the featural filling-in process. A boundary completion signal (to be detailed in Sec. III.B) with leakage was used to keep the diffusion process inside the square. However, in this example, the diffusion flow leaks through the gaps and spreads across the entire surface.

#### B. Boundary Completion System

The boundary completion signals (signal generated by boundary completion system) define the region in which the diffusive filling-in process does apply. These signals thus act as algorithm blockers, which prevent the propagation of the diffusion flow out of a particular perceptual region. In the boundary completion system, the input signal (according to Fig. 5) is processed through four stages [10]: oriented filtering, spatial competition, orientation competition, and bipole grouping.

*Oriented filtering* is a very well-known characteristic of the visual system. It has been confirmed both anatomically and physiologically. Orientation filters implemented at the cortical level take part in higher-level segmentation functions. *Spatial competition* is the mechanism through which the input responses have their edges enhanced by means of a Laplacian filter that weighs a central pixel against its neighboring pixels. The *orientation competition* stage preserves strong signals with clearly defined orientation coming up from the spatial competition stage. This stage inhibits weaker orientation signals, so that the next stage can form coherent groups. The name *bipole* is used in [10] to represent a filter (also termed a *kernel*) upon which the *bipole grouping* stage is based. In particular, the term *bipole* is applied to a filter that models a specific connection between three or more cells at the visual cortex. One of these cells, called the output cell, yields output equal to logical 1 only if it receives enough excitatory input

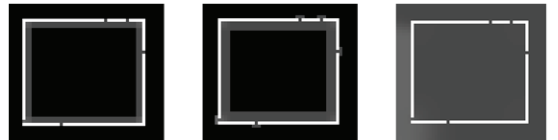


**Figure 6.** Example of diffusive filling-in process. In this example, the diffusion flow escapes through the holes.

simultaneously from both input cells. For simplicity, the output cell also receives the same name: bipole. Bipole grouping is the main stage in the boundary completion process and it will be described in more detail in the sequel. The first three stages of the boundary completion system are not discussed here, but further information about them can be found in [10].

Bipole grouping performs a long-range cooperation within one given orientation, and a short-range competition between different orientations, in order to extrapolate lines and thus connect parts of the stimulus which might belong to the same object [7]. Long-range cooperation happens when the bipole output cell receives a connection from orientation filter cells that are far away. The bipole output completes the missing points among two previously disconnected segments. Short-range competition happens between segments with different orientation in the same position, so that the segments with less luminance are removed. Considering the *On Lum* and *Off Lum* inputs (Fig. 5) we can state that, if a pixel is not associated with segments to be connected (even if the segments have different orientation), then the corresponding bipole (filter) output will not be activated. Filters that are used in the bipole grouping operation can be found in [8] and a very compact one-dimensional example is shown in Eq. (2). The vectors  $B_C$ ,  $B_E$ , and  $B_D$  are examples of components of a bipole that operates on the spatial scale of three pixels. The  $\varepsilon$  factor is a scale constant and  $x$  represents the input signal (*On Lum* and *Off Lum* according to Fig. 5). The expression  $x*B$  denotes convolution between  $x$  and  $B$ .

$$\begin{aligned} B_C &= [1 \ 0 \ 1] \\ B_E &= [1 \ 0 \ 0] \\ B_D &= [0 \ 0 \ 1] \end{aligned}$$

$$BP[x] = x * B_C - \left( \frac{\varepsilon \cdot x * B_E}{x * B_D + \varepsilon} + \frac{\varepsilon \cdot x * B_D}{x * B_E + \varepsilon} \right) \quad (2)$$

In [10], the bipole grouping operator might interact with segments having different orientations and it has a particular spacial arrangement that allows grouping of curved line segments. For simplicity, we consider at this point only equally-oriented straight-line segment grouping. In Fig. 7, an input signal  $x(n)$  undergoes convolution with the  $B_C$  filter  $[1 \ 0 \ 0 \ 0 \ 1]$ ,  $B_E$  filter  $[1 \ 0 \ 0 \ 0 \ 0]$ , and  $B_D$  filter  $[0 \ 0 \ 0 \ 0 \ 1]$ , with  $\varepsilon = 0.01$ . The boundary response  $y(n)$  is non-zero only if both convolutions results (from  $B_E$  and  $B_D$ ) are larger than zero.

If gaps with different sizes are present, then, to make the union of separate segments of a straight line possible, bipoles at different spatial scales must be used. The largest spatial scale of a bipole is associated with the maximum size of an admissible gap between two segments to be grouped.

To create bipoles adjusted to different orientations, the  $B_C$ ,  $B_E$  and  $B_D$  filters must be rotated to the proper orientations. In Eq. (3), we show simple examples of the BC filter represented at  $0^\circ$  and  $90^\circ$  rotations. If the *On Lum* and *Off Lum* information is processed by an orientation filter  $f(\theta)$ , then this

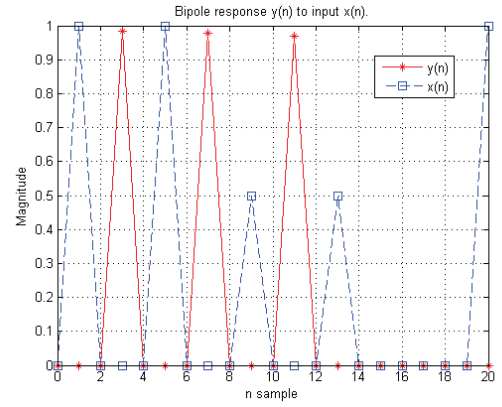


**Figure 7.** Illustration of a bipole function implementing a logical AND operation among its neighbors. In this figure, a straight line segment such as the ones in Fig. 8 is seen from a longitudinal point-of-view.

$$B_C^{(0^\circ)} = \begin{bmatrix} 0 & 0 & 0 \\ 1 & 0 & 1 \\ 0 & 0 & 0 \end{bmatrix}, \quad B_C^{(90^\circ)} = \begin{bmatrix} 0 & 1 & 0 \\ 0 & 0 & 0 \\ 0 & 1 & 0 \end{bmatrix} \quad (3)$$

part of the potential boundary information can only be detected by a bipole that is tuned to an orientation represented by  $\theta$ . Equation (4) shows an orientation *mask* (filter) corresponding to  $\theta = 90^\circ$ . Information is indeed propagated into higher regions of the visual cortex by means of separated channels. In some parts of the visual cortex, orientation serves as a separation criterion.

$$f_{90^\circ} = \begin{bmatrix} -1 & 1 & -1 \\ -1 & 1 & -1 \\ -1 & 1 & -1 \end{bmatrix} \quad (4)$$

To illustrate the operation of the bipole stage, Fig. 8 shows the result that is obtained when Eq. (4) is applied to the image of a square that is incomplete because of the presence of some gaps. The right side of Fig. 8 shows the result of the bipole operation ( $\theta = 90^\circ$  and filter size  $7 \times 7$ ) applied to the center of Fig. 8. The response is shown only for positive values. Negative values are changed to zero, since magnitude values are represented by neuron firing rates.

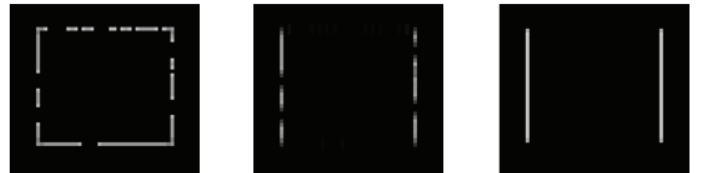


**Figure 8.** Illustration of the bipole grouping operation: square before segmentation (left); square components at  $90^\circ$  orientation before being processed by the bipole (center); and after processing (right).

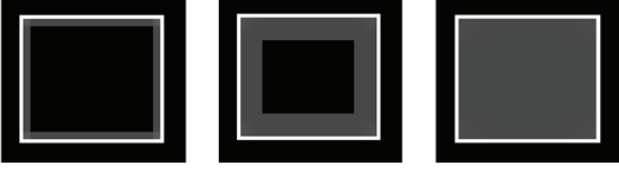


**Figure 9.** Diffusive filling-in process applied to a boundary contour system without leakage: input (left), diffusion start (center) and diffusive filling-in result (right).

In Fig. 9, the boundary signal does not have any hole, thus the diffusion flow is maintained inside the square. It is important to note that boundary contour signal does not correspond to visual perception itself.

#### IV. RESULTS

The generation of the simulation results that are presented in this section is based on Eqs. (5), (6), (7) and (8). The implementation of the boundary completion system along each orientation  $\theta$  is described by Eqs. (5) and (6) (*on* and *off* pathways respectively). The featural filling-in system, is based on Eqs. (7) and (8), also associated with *on* and *off* pathways.

In Eqs. (5) and (6),  $y(n)$  is an output signal,  $f(\theta)$  denotes a convolution operation performed by a filter tuned to orientation  $\theta$ , and  $BP$  is the bipole grouping operation, also at orientation  $\theta$ , which is described by Eq. (2). In Eqs. (7) and (8),  $w(n)$  is the output signal, the *On Lum* and *Off Lum* signals represent input information that is coming from the retina (Fig. 3), and  $F$  is the diffusive operation described in Eq. (1). Although other orientations and other stages of the boundary completion system could have been used, in the present work we consider only  $0^\circ$  and  $90^\circ$  orientations, for simplicity. In Eqs. (5) to (8), the (+) symbol indicates that the only positive values are considered in the response. Negative values are discarded.

$$y_{(n+1)}^{(\theta)}{}_{On} = BP^{(\theta)+} [f^{(\theta)+} [On_{Lum}] + y_{(n)}^{(\theta)}{}_{On}] \quad (5)$$

$$y_{(n+1)}^{(\theta)}{}_{Off} = BP^{(\theta)+} [f^{(\theta)+} [Off_{Lum}] + y_{(n)}^{(\theta)}{}_{Off}] \quad (6)$$

$$w_{(n+1)On} = F^+ [On_{Lum} + w_{(n)On} - \sum_{\theta} y^{(\theta)+}{}_{Off}] \quad (7)$$

$$w_{(n+1)Off} = F^+ [Off_{Lum} + w_{(n)Off} - \sum_{\theta} y^{(\theta)+}{}_{On}] \quad (8)$$

Rather than using bipole filters with different lengths, we use a compact format shown in Eq. (9). Figure (10) shows that, by applying Eq. (5) to vertical stripes that are separated by three pixels in a cross-sectional view (blue lines), a boundary contour (red segment) is obtained as a result.

By applying a two-dimensional version of the filters shown in Eq. (9), a similar result is achieved for a filling-in

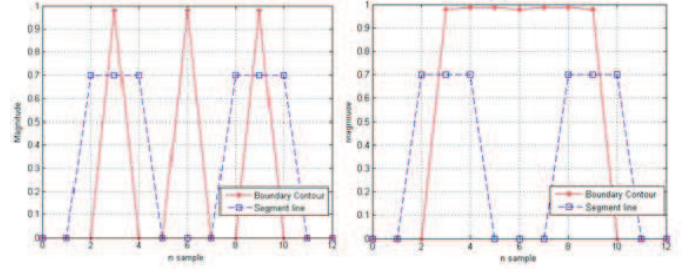


**Figure 10.** Boundary completion system merging two line segments (cross-sectional view). The horizontal axis represents the pixel position and the vertical axis indicates the luminance. The first iteration is shown on the left. The boundary completion system generates a signal that connects the two segments of a line, after some iterations (right).

$$\begin{aligned} B_C &= [1110111] \\ B_E &= [1110000] \\ B_D &= [0000111] \end{aligned} \quad (9)$$

problem defined over two dimensions. The image is split into two parts by filters with  $0^\circ$  and  $90^\circ$  orientations. Each part is processed by a bipole adjusted to the same orientation. The signal that blocks the diffusion flow is composed by the sum response signals that are generated by the boundary completion system (sign-oriented at  $0^\circ$  and  $90^\circ$ ). The input and output of the boundary completion system are shown in Fig. 11.

The filling-in process occurs over both *on* and *off* channels and the visual perception is represented by the difference between the results. The *on* channel filling-in processing is illustrated by Fig. 12. In the first row, we can see the image to be processed by the early visual system (left), the image with information loss caused by the blind spot (center), and the result of early visual system processing applied to the lossy data (right). The top-right image must be used to recover the original image. A similar version of this top-right image, but coming from the *off* channel, is fed to the *on* input of the boundary completion system. The boundary signal result is shown in the first column of the second row: this signal represents a completely closed curve, which is suitable for diffusive filling-in without any leakage. The diffusion process result (after a few iterations) appears in the center image, and the final result is shown in the rightmost image, together with the boundary contour signal shown in light gray.

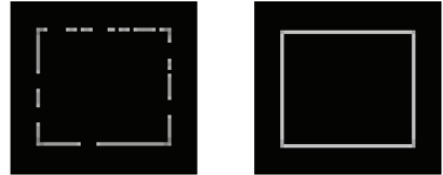


**Figure 11.** Boundary completion system merging several straight line segments in two orientations ( $0^\circ$  and  $90^\circ$ ).

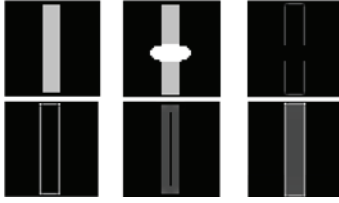


**Figure 12.** Various stages of diffusive filling-in for an image that has suffered loss of information in the early visual system due to DoG filtering and blind spot.

## V. INTEGRATE-AND-FIRE ALGORITHM

Networks build upon IF neurons can solve computer vision problems efficiently and in real time [15]. They can also be used for pattern recognition applications. It is important to mention them in this work, because of their compatibility with biological systems. Equation (10) describes the charging of  $C_m$ , which represents the membrane capacitance of a cell. The membrane instantaneous voltage is  $V_m$ . The constant values  $V_E$  and  $V_I$  determine the maximum and minimum membrane voltages. Conductances  $g_E$  and  $g_I$  model excitatory and inhibitory inputs. The membrane voltage increases or decreases accordingly. When  $V_m$  exceeds a threshold  $V_{TH}$ , a spike is generated and then  $V_m$  is reset. The settling time  $\tau$  and the firing rate  $f_{out}$  of the cell are indicated in (11) and (12). An IF model for diffusive filling-in can be proposed from Eqs. (10) to (12). A simple bipole model is shown in Fig. 13. Dashed lines indicate inhibition and solid line indicate excitation. The bipole tends to complete the center information in patters of 1-0-1 type to 1. For other patterns, the center is not completed. In Fig. 14, the IF model is applied to featural filling-in. Information exchange among cells occurs laterally, and a boundary completion system layer blocks signal propagation at the diffusive layer.

$$C_m \frac{dV_m}{dt} = (V_E - V_m) \cdot g_E + (V_m - V_I) \cdot g_I \quad (10)$$

$$\tau \approx \frac{5 \cdot C_m}{g_E - g_I} \quad (11)$$

$$f_{out} \approx \frac{V_E}{\tau \cdot V_{TH}} \quad (12)$$

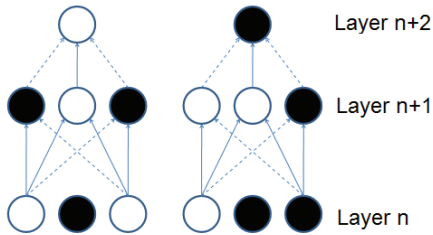


**Figure 13.** Implementation of an AND gate using IF neurons. White circles indicate cell activity and black circles indicate its absence. When both its sides have activity, the center cell is activated (left). Otherwise, the center cell is off (right).

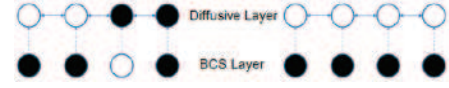


**Figure 14.** Diffusive filling-in. Layer activity occurs laterally between cells of the same layer. Left: filling-in is blocked by an activity boundary completion system layer. Right: filling-In flows freely between diffusive layer cells.

## VI. CONCLUSION

We presented a novel study of diffusive filling-in – an algorithm that runs in the visual cortex – taking into account the way signals from the early visual system are used by the algorithm. A model showing the related signals and features of the early visual system was presented. Hardware to implement parts of the early visual system is under construction and we plan to integrate it with the diffusive filling-in algorithm. We presented system-level test results showing that the filling-in algorithm is suitable for the integration. We also discussed the implementation of this algorithm using IF neuron models. Further studies of IF neuron models are useful for the hardware implementation of the diffusive filling-in algorithm.

## REFERENCES

- [1] A. Andreou and K. Boahen, "A 48,000 pixel, 590,000 transistor silicon retina in current-mode subthreshold CMOS", Proc. 37th Midwest Symp. Circ. Syst., vol. 1, pp. 97-98, Aug. 1995.
- [2] K. Boahen, "A retinomorph chip with parallel pathways", Analog Integrated Circ. and Signal Proc., vol. 30, pp. 121-135, Feb. 2002.
- [3] E. Chicca and G. Indiveri, "A multichip pulse-based neuromorphic infrastructure and its application to a model of orientation selectivity", IEEE Trans. Circ. Syst. I, vol. 54, May 2007.
- [4] C. Enroth-Cugell and J. G. Robson, "The contrast sensitivity of retinal ganglion cells of the cat", J. Physiol., vol. 187, pp. 517-552, Dec. 1966.
- [5] R. Rodieck, "Quantitative analysis of cat retinal ganglion cell response to visual stimuli", Elsevier Vision Research, pp. 583-601, Dec. 1965.
- [6] D. Marr, "Vision: a computational investigation into the human representation and processing of visual information", New York, 1982.
- [7] S. Grossberg, "Cortical dynamics of three-dimensional form, color, and brightness perception", Percept. Psychophys, vol. 41, pp. 87-116, 1995.
- [8] A. Gove, S. Grossberg and E. Mingola, "Brightness perception, illusory contours and corticogeniculate feedback", Visual Neuroscience, vol. 12, pp. 1027-1052, 1995.
- [9] K. Stingl et al., "Artificial vision with wirelessly powered subretinal electronic implant alpha-IMS", Proc. R. Soc. B, vol. 280, Feb. 2013.
- [10] S. Grossberg, L. Kuhlmann and E. Mingola, "A neural model of 3D shape-from-texture: multiple-scale filtering, boundary grouping, and surface filling-in", Visual Res. Pub. Med., vol 47, Feb. 2007.
- [11] H. Neumann et al., "Visual filling-in for computing perceptual surface properties", Biol. Cybern. Pub. Med., vol. 85, Nov. 2001.
- [12] E. Culurciello, E. Cummings, and K. Boahen, "High dynamic range, arbitrated address event representation digital imager", IEEE Int. Symp. Circ. Syst., vol. 2, pp. 505-508, May 2001.
- [13] L. Mesa and L. Barranco, "An event-driven multi-kernel convolution processor module for event-driven vision sensors", IEEE J. Solid-State Circ., vol. 47, pp. 504-517, Feb. 2012.
- [14] M. Fiorani, M. Rosa, R. Gattass and C. Miranda, "Dynamic surround of receptive fields in primate striate cortex: a physiological basis for perceptual completion?", Proc Natl. vol. 89: pp. 8547-8551, Sep. 1992.
- [15] W. Maass, "Networks of Spiking Neurons: The Third Generation of Neural Network Models", Elsevier Neural Networks, vol. 10, pp. 1659-1671, Jun. 1997.